



*Supplement of*

## **Controls of aeolian and fluvial sediment influx to the northern Red Sea over the last 220 000 years**

**Werner Ehrmann et al.**

*Correspondence to:* Werner Ehrmann (ehrmann@uni-leipzig.de)

The copyright of individual parts of the supplement might differ from the article licence.

## Clay mineral analyses

The description of the method is reproduced from Ehrmann and Schmiedl, 2021: “We treated freeze-dried bulk sediment samples with 3% hydrogen peroxide and 10% acetic acid in order to remove organic and calcareous components, and then separated the clay (<2 µm) from the coarse fraction in settling tubes. 40 mg of suspended clay was mixed with 1 ml of a 0.04% MoS<sub>2</sub> suspension and filtered through a membrane filter with 0.20 µm pore width. We dried the filter cakes at 60°C and mounted them on aluminium tiles. The mounts were exposed to ethylene-glycol vapour at a temperature of 60°C for at least 18 hours immediately before the measurements. XRD analyses were conducted on a diffractometer system Rigaku Miniflex with CoK $\alpha$  radiation (30 kV, 15 mA) in the range 3–40°2 $\Theta$  (step size 0.02°2 $\Theta$ , measuring time 2 sec/step). Additionally, we measured the range 27.5–30.6°2 $\Theta$  in higher resolution (step size 0.01°2 $\Theta$ , measuring time 4 sec/step) in order to better resolve the (002) peak of kaolinite and the (004) peak of chlorite. We evaluated the X-ray diffractograms using the interactive “MacDiff” software (Petschick, 2001). After adjusting the diffractograms to the MoS<sub>2</sub> peak at 6.15 Å, we identified the main clay minerals by their basal reflections at 17 Å (smectite), 10 and 5 Å (illite), 14.2, 7, 4.72 and 3.54 Å (chlorite), 7 and 3.58 Å (kaolinite), and 10.5 Å (palygorskite). We deconvoluted the peak doublets smectite/chlorite (17/14 Å), palygorskite/illite (10.5/10 Å) and kaolinite/chlorite (3.58/3.54 Å). Semi-quantitative evaluations of the clay mineral assemblages were performed on the integrated peak areas, using empirically estimated weighting factors (Biscaye, 1964, 1965; Weaver and Beck, 1977).”

## Grain size analyses

Freeze-dried bulk sediment samples were treated with 10% acetic acid and 3% hydrogen peroxide to remove carbonate and organic carbon, respectively. Grain size analyses were performed using a Laser Particle Sizer (Analysette 22, Fritsch GmbH). For each sample, we made four consecutive measurements of their grain size distributions and calculated their mean. The percentages of clay, silt and sand were calculated, as well as the mean grain size of each sample.

## XRF core scanning

Prior to scanning, the core was smoothed and covered with a 4-µm-thick Ultralene® X-ray transmission foil in order to avoid potential contamination and desiccation of the sediment. We measured major and trace elements of KL23 at the Leibniz-Institut für Ostseeforschung, Warnemünde, Germany, with an ITRAX (Cox Analytical Systems) X-ray fluorescence (XRF) core scanner, equipped with a Cr-tube running with a tube voltage of 30 kV and a tube current of 55 mA. The exposure time was 5 ms per measurement and the scanning interval was 0.2 cm. No data for calibrating and correcting for water content were available.

## Analyses of radiogenic isotopes

We treated our samples to remove all authigenic marine contaminants from the isotope fingerprint of the terrigenous fraction (carbonate, authigenic Fe-Mn oxyhydroxide coatings, organic carbon and marine barite) using the method of Jewell et al. (2022). That study demonstrated that small quantities of marine barite can have a large contaminating effect on the isotopic composition of the terrigenous fraction, especially for Sr. To remove marine barite, samples were leached with 0.2 M diethylene triamine pentaacetic acid (DTPA) in 2.5 M NaOH and left in a water bath set to 80 °C for 30 minutes. Following the recommended treatment protocol in Jewell et al. (2022), we repeated this step four times on three test samples to determine how many treatments were optimal for complete barite removal at this site. Marine sediments were considered free of marine barite when there was no appreciable decrease in Sr or Ba concentration, and no further change in measured  $^{87}\text{Sr} / ^{86}\text{Sr}$  of the silicate fraction with additional DTPA-NaOH treatment. Based on our test samples, we employed one DTPA-NaOH treatment (following the removal of all other marine phases).

Our column chemistry procedure followed Jewell et al. (2022). Major element concentrations of sample residues were determined using a ThermoFisher iCAP6500 dual view inductively coupled plasma optical emission spectrometer (ICP-OES). Trace element concentrations were measured using quadrupole inductively coupled plasma mass spectrometer (ICP-MS Thermo Fisher Scientific XSeries 2). A suite of international rock standards was used for calibration (JB-1a, JGb-1, JB-2, JB-3, BHVO2, AGV-2, BCR-2, BIR-1), plus a spike of 5 ppb In, 5 ppb Re & 20 ppb Be as an internal standard. The precision for all measurements was <5.6 %.

After column separation, the Sr fraction was dried down and loaded onto an outgassed tantalum filament with 1ml of a tantalum activator solution. The samples were analysed using a Thermo Fisher Scientific Triton Thermal Ionisation Mass Spectrometer using a multidynamic procedure and an  $^{88}\text{Sr}$  beam of 2V. Fractionation was corrected using an exponential correction normalised to  $^{86}\text{Sr} / ^{88}\text{Sr} = 0.1194$ . NIST987 was run as a standard in each turret and over the course of this study  $^{87}\text{Sr} / ^{86}\text{Sr} = 0.710241 \pm 0.000008$  (2sd; n = 20). The long-term average for NIST987 on this instrument is  $0.710242 \pm 0.000021$  (2sd; n = 531).

Nd-isotope ratios were measured using a multi-collector ICP-MS (MC-ICP-MS, Thermo Fisher Scientific Neptune). Nd isotopic compositions were corrected following the method of Vance and Thirlwall (2002) through adjustment to a  $^{146}\text{Nd} / ^{144}\text{Nd}$  ratio of 0.7219 and a secondary normalisation to  $^{142}\text{Nd} / ^{144}\text{Nd} = 1.141876$ . For convenience the Nd isotope ratios are reported in epsilon notation ( $\epsilon_{\text{Nd}}$ ), where  $^{143}\text{Nd} / ^{144}\text{Nd}_{\text{CHUR}}$  represents the Chondrite Uniform Reservoir (CHUR) value of 0.512638 (Jacobsen and Wasserburg, 1980), following Eq. (1):

$$\epsilon_{\text{Nd}} = \left[ \frac{^{143}\text{Nd} / ^{144}\text{Nd}_{\text{sample}}}{^{143}\text{Nd} / ^{144}\text{Nd}_{\text{CHUR}}} - 1 \right] \times 10^4 \quad (1)$$

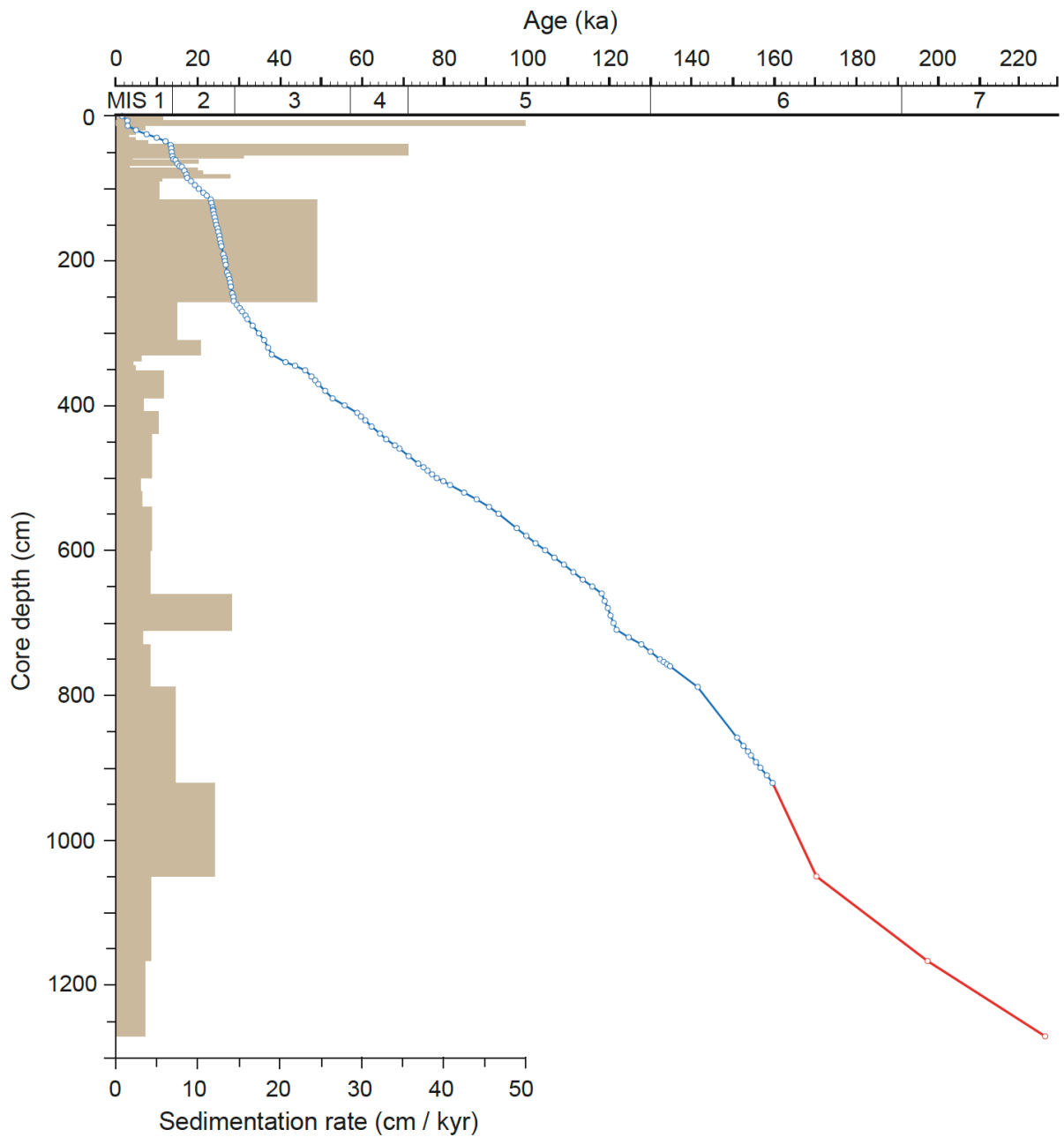


**Figure S1.** Age / depth plot with calculated sedimentation rates for sediment core KL23. The age model of the interval from 0 to 920 cm (blue line) is based on the correlation of the planktic foraminiferal and Soreq speleothem  $\delta^{18}\text{O}$  records and integration of eight AMS radiocarbon dates (Hartman et al., 2020). The age model of the interval from 920 to 1260 cm (red line) is based on the benthic foraminiferal  $\delta^{18}\text{O}$  record (Geiselhart, 1998) and the Red Sea sea-level record (Grant et al., 2014).

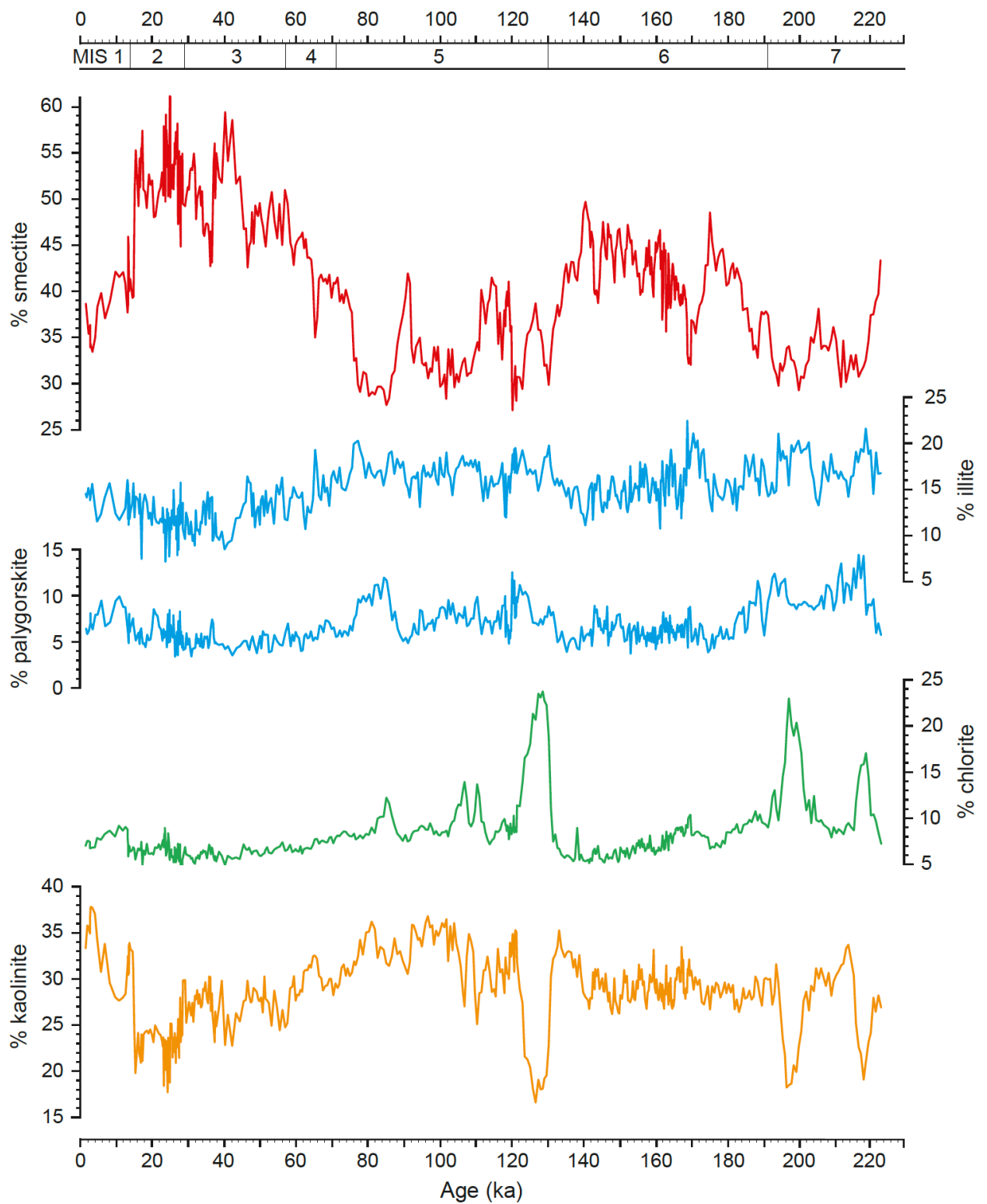


**Figure S2.** Clay mineral composition of sediments from core KL23. Marine isotope stages (MIS) are indicated at the top.

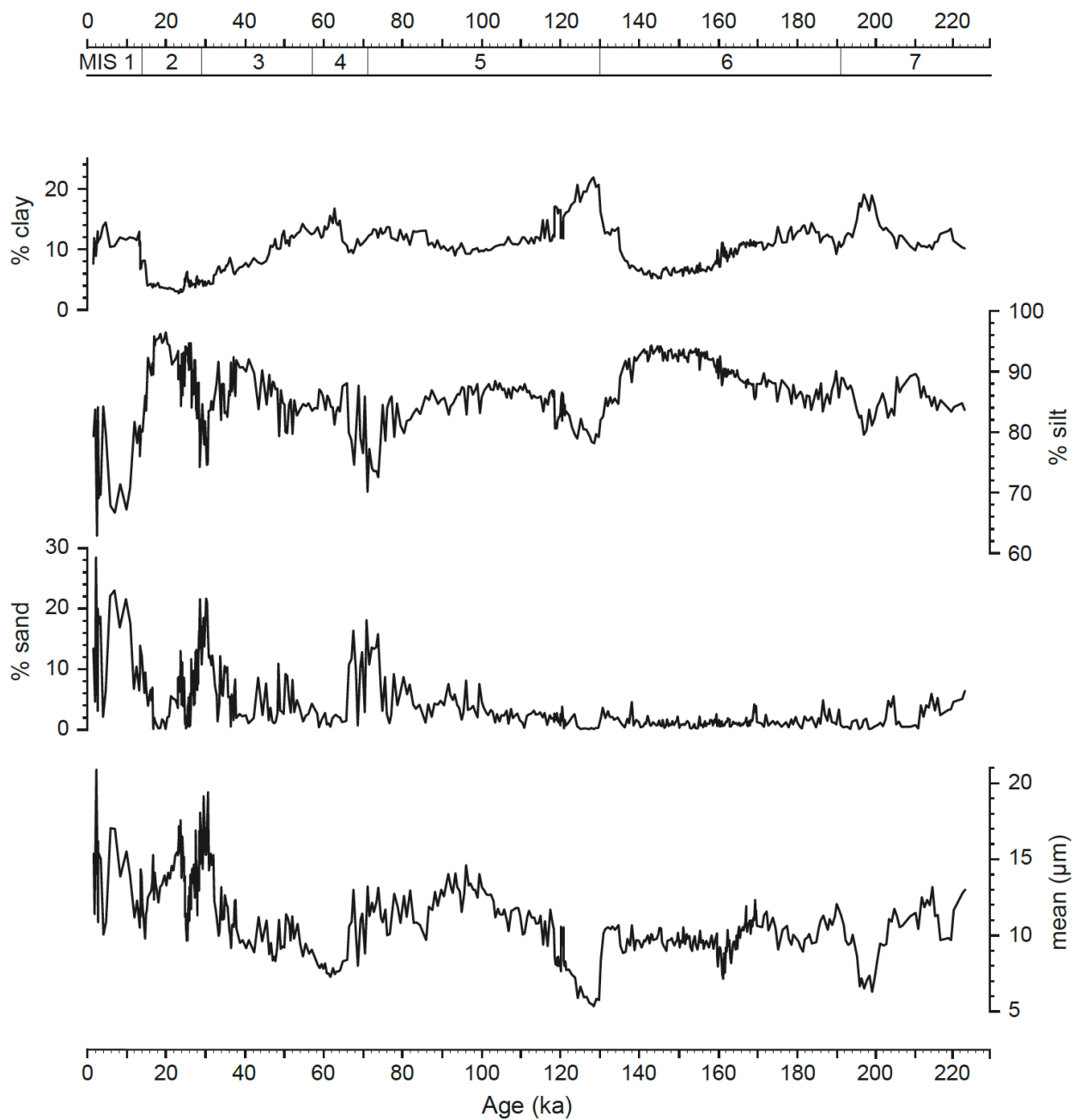


**Figure S3.** Grain size data from the terrigenous sediment components of core KL23: percentages of clay (<math><2\ \mu\text{m}</math>), silt (<math>2\text{--}63\ \mu\text{m}</math>), and sand (><math>63\ \mu\text{m}</math>), and mean grain size (<math>\mu\text{m}</math>). Marine isotope stages (MIS) are indicated at the top.

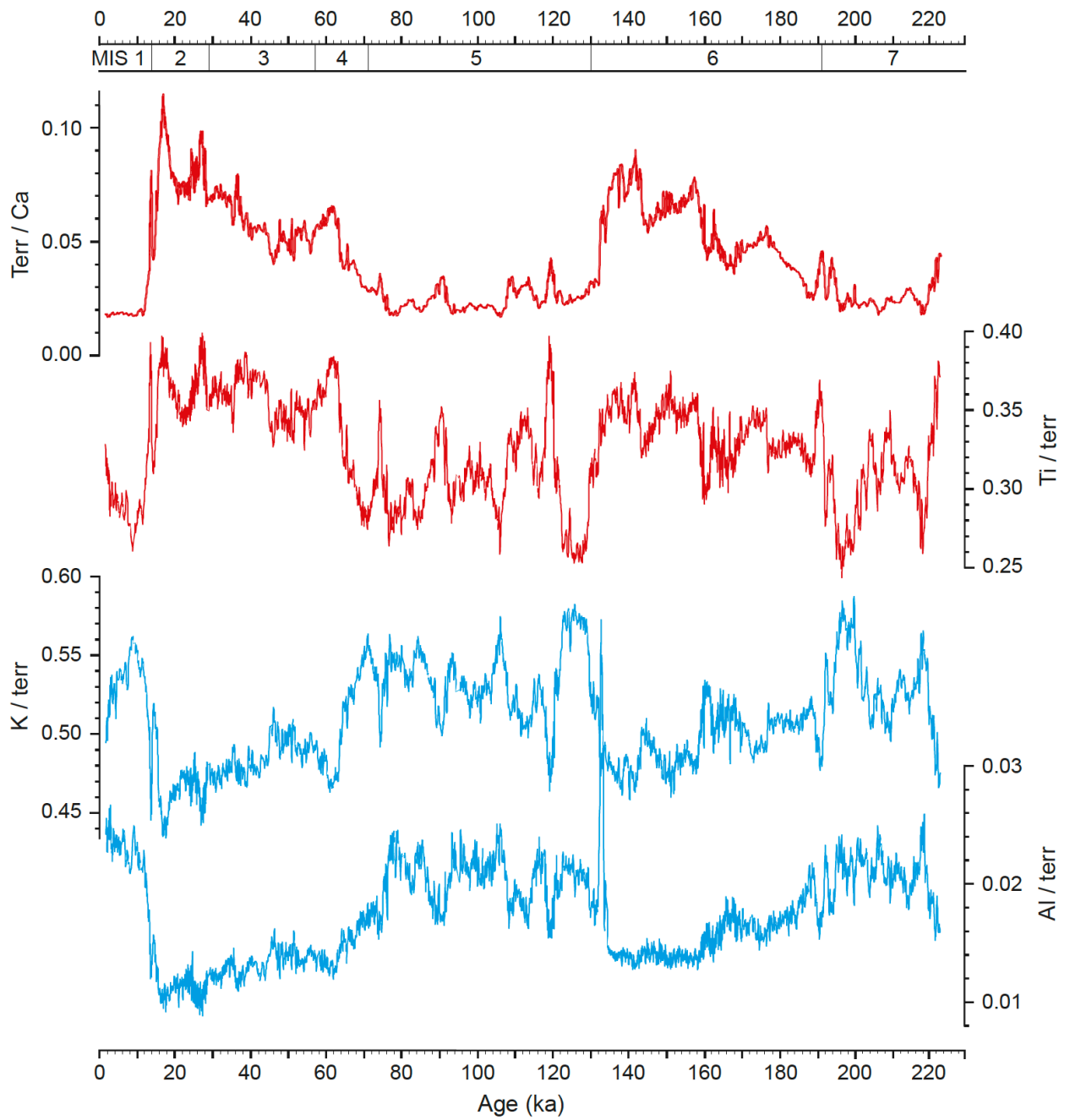


**Figure S4.** XRF sediment geochemistry from core KL23 (five-point running average). Terr / Ca gives the ratio between the sum of terrigenous elements and Ca. Ti, K, and Al were normalized by calculating their portion on the terrigenous elements. Marine isotope stages (MIS) are indicated at the top.

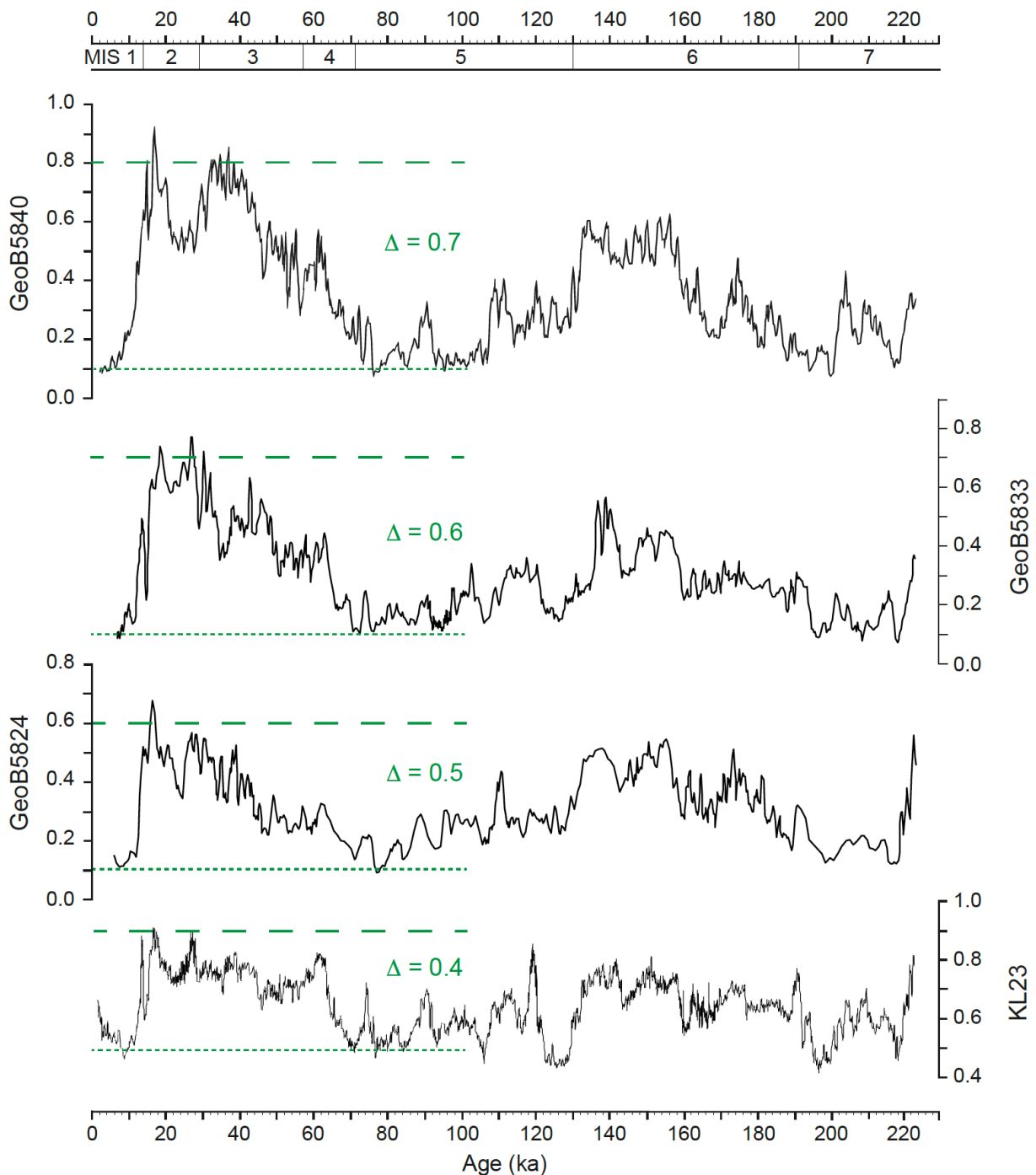


**Figure S5.** Ti / K ratios from XRF core scanning along a N-S core transect in the northern Red Sea. Data from GeoB cores are from Arz et al. (2001). XRF data are stored in the Pangaea data base (<https://doi.org/10.1594/PANGAEA.90845>; <https://doi.org/10.1594/PANGAEA.90846>, and <https://doi.org/10.1594/PANGAEA.90848>). The age models of the GeoB cores have been tuned to KL23 starting with the initial stratigraphies as provided in Arz et al. (2001) and performing subsequent graphical finetuning of the XRF Ti / K ratios with QAnalySeries (Kotov and Pälike, 2018). Marine isotope stages (MIS) are indicated at the top.

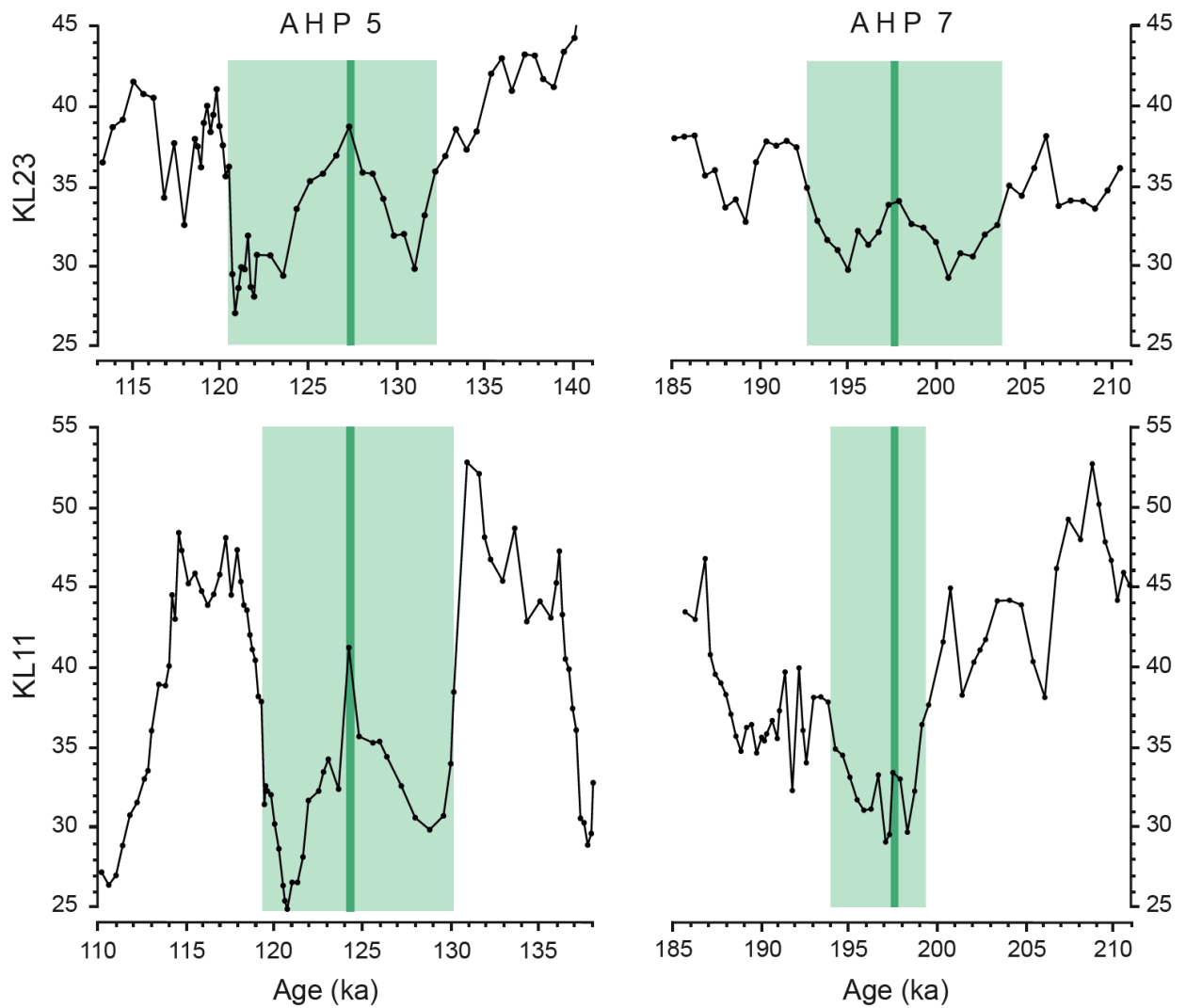


**Figure S6.** Smectite concentrations in core KL23 from the northern Red Sea and KL11 from the central Red Sea for intervals including AHP5 (left) and AHP7 (right). The AHPs are marked by green shading, the peak humid phases by a green line. Data for KL11 are from Ehrmann et al. (2024). The different timing of the AHPs is probably due to inconsistencies in the age models.

## References

- Arz, H. W., Pätzold, J., Moammar, M. O., and Röhl, U.: Late Quaternary climate records from the northern Red Sea: results on gravity cores retrieved during R/V METEOR Cruise M44/3, *K. KAU: Mar. Sci.*, 12, 101–113, [https://www.kau.edu.sa/files/320/researches/51790\\_21923.pdf](https://www.kau.edu.sa/files/320/researches/51790_21923.pdf), 2001.
- Biscaye, P. E.: Distinction between kaolinite and chlorite in recent sediments by X-ray diffraction, *American Mineralogist*, 49, 1281–1289, [https://msaweb.org/AmMin/AM49/AM49\\_1281.pdf](https://msaweb.org/AmMin/AM49/AM49_1281.pdf) (last access 23 February 2025), 1964.
- Biscaye, P. E.: Mineralogy and sedimentation of recent deep-sea clay in the Atlantic Ocean and adjacent seas and oceans, *Geol. Soc. Am. Bull.*, 76, 803–832, [https://doi.org/10.1130/0016-7606\(1965\)76\[803:MASORD\]2.0.CO;2](https://doi.org/10.1130/0016-7606(1965)76[803:MASORD]2.0.CO;2), 1965.
- Ehrmann, W. and Schmiedl, G.: Nature and dynamics of North African humid and dry periods during the last 200,000 years documented in the clay fraction of Eastern Mediterranean deep-sea sediments, *Quaternary Sci. Rev.*, 260, 106925, <https://doi.org/10.1016/j.quascirev.2021.106925>, 2021.
- Ehrmann, W., Wilson, P. A., Arz, H. W., Schulz, H., and Schmiedl, G.: Monsoon-driven changes in aeolian and fluvial sediment input to the central Red Sea recorded throughout the last 200 000 years, *Clim. Past*, 20(1), 37–52, <https://doi.org/10.5194/cp-20-37-2024>, 2024.
- Geiselhart, S.: Late Quaternary paleoceanographic and paleoclimatic history of the Red Sea during the last 380,000 years: evidence from stable isotopes and faunal assemblages, PhD Thesis, *Tübinger Mikropaläontol. Mitt.*, 17, 1–87, ISSN 0935-493 X, 1998.
- Grant, K. M., Rohling, E. J., Ramsey, C. B., Cheng, H., Edwards, R. L., Florindo, F., Heslop, D., Marra, F., Roberts, A. P., Tamisiea, M. E., and Williams, F.: Sea-level variability over five glacial cycles, *Nat. Commun.*, 5, 5076, <https://doi.org/10.1038/ncomms6076>, 2014.
- Hartman, A., Torfstein, A., and Almogi-Labin, A.: Climate swings in the northern Red Sea over the last 150,000 years from  $\epsilon_{\text{Nd}}$  and Mg/Ca of marine sediments, *Quaternary Sci. Rev.*, 231, 106205, <https://doi.org/10.1016/j.quascirev.2020.106205>, 2020.
- Jacobsen, S. B. and Wasserburg, G. J.: Sm-Nd isotopic evolution of chondrites, *Earth Planet. Sci. Lett.*, 50(1), 139–155, [https://doi.org/10.1016/0012-821X\(80\)90125-9](https://doi.org/10.1016/0012-821X(80)90125-9), 1980.
- Jewell, A. M., Cooper, M. J., Milton, J. A., James, R. H., Crocker, A. J., and Wilson, P. A.: Chemical isolation and isotopic analysis of terrigenous sediments with emphasis on effective removal of contaminating marine phases including barite, *Chem. Geol.*, 589, 120673, <https://doi.org/10.1016/j.chemgeo.2021.120673>, 2022.
- Kotov, S. and Pälke, H.: QAnalySeries – a cross-platform time series tuning and analysis tool, AGU, <https://ui.adsabs.harvard.edu/abs/2018AGUFMPP53D1230K/abstract>, 2018.
- Petschick, R.: MacDiff 4.2.5. [https://www.uni-frankfurt.de/69528130/Petschick\\_\\_\\_MacOS\\_Software](https://www.uni-frankfurt.de/69528130/Petschick___MacOS_Software) (last access: 23 February 2025), 2001.
- Vance, D. and Thirlwall, M.: An assessment of mass discrimination in MC-ICPMS using Nd isotopes, *Chem. Geol.*, 185(3–4), 227–240, [https://doi.org/10.1016/S0009-2541\(01\)00402-8](https://doi.org/10.1016/S0009-2541(01)00402-8), 2002.
- Weaver, C. E. and Beck, K. C.: Miocene of the S.E. United States: A model for chemical sedimentation in a peri-marine environment, *Sed. Geol.*, 17, 1–234, [https://doi.org/10.1016/0037-0738\(77\)90062-8](https://doi.org/10.1016/0037-0738(77)90062-8), 1977.